

## Simulação Numérica de Inundações em Casos de Rompimento de Barragem

### *Numerical Simulation of Flooding in Dam-break Cases*

Rafael Zanovelo Perin<sup>1</sup>, Régis Sperotto de Quadros<sup>2</sup>, Armando Miguel Awruch<sup>3</sup>

#### RESUMO

A água é um recurso fundamental para o desenvolvimento da sociedade, atraindo as comunidades desde o início da civilização. Esta proximidade das civilizações dos recursos hídricos demandou estratégias para uma melhor gestão da água, como a construção de barragens, sujeitando os ecossistemas a problemas mais graves. Neste trabalho, as equações de águas rasas são resolvidas numericamente pelo método dos elementos finitos e o método das linhas ou direções características, no espaço e no tempo, respectivamente. O modelo é utilizado para simular casos de rompimento de barragem encontrados na literatura, em leito molhado sem obstáculos e com obstáculos sólidos. Os resultados obtidos estão em conformidade com as publicações, validando a metodologia adotada. Por fim, as simulações numéricas possibilitam conhecer a ocorrência do escoamento de rompimento de barragem, gerando informações acerca da ocorrência deste tipo de evento desastroso.

**Palavras-chave:** Sistemas de águas rasas. Método dos elementos finitos. Método das linhas ou direções características.

#### RESUMO

Water is a fundamental resource for the development of society, attracting communities since the beginning of civilization. This proximity of civilizations to water resources has demanded strategies for better water management, such as the construction of dams, subjecting ecosystems to more serious problems. In this paper, the shallow water equations are solved numerically by the finite element method and the characteristic-based split scheme, in space and time, respectively. The model's used to simulate dam-break cases from literature, in wet bed without obstacles and with solid obstacles. The results obtained are in accordance with the publications, validating the adopted methodology. Finally, the numerical simulations make it possible to know the occurrence of dam-break flow, generating information about the occurrence of this kind of disastrous event.

**Keywords:** Shallow water systems. Finite element method. Characteristic-based split scheme.

<sup>1</sup> Mestre em Modelagem Matemática pela Universidade Federal de Pelotas. ORCID: <https://orcid.org/0000-0002-7671-8372>;

E-mail: [rafael-perin@hotmail.com](mailto:rafael-perin@hotmail.com)

<sup>2</sup> Doutor em Matemática Aplicada pela Technische Universität Darmstadt. Professor e coordenador do Programa de Pós-graduação em Modelagem Matemática da Universidade Federal de Pelotas. ORCID: <https://orcid.org/0000-0002-9720-8013>;

<sup>3</sup> Doutor em Engenharia Civil pela Universidade Federal do Rio de Janeiro. Professor visitante do Programa de Pós-graduação em Modelagem Matemática da Universidade Federal de Pelotas. ORCID: <https://orcid.org/0000-0002-7651-3414>.

## 1. INTRODUCTION

Water is a natural resource of reference for the prosperity and maintenance of society, so that it encouraged civilizations to stay close to water resources. This proximity to water left the communities subject to the adversities coming from the environment, as in the case of water shortage, floods, pollution, tsunamis and others (CARDOSO, 1980).

Social demands were added to the growth of cities and urbanization, leading to an increase in the use of water for the support of urban areas and the development of services. It's necessary to build dams, dikes, industries, and power plants for a better utilization and management of water resources.

These constructions satisfy the people's needs at the same time subjecting different ecosystems to even more severe disasters, whether from the uncontrolled increase of pollutants or the dam-break cases, which can be triggered by human factors or natural causes. Thus, even as fundamental, water becomes an even greater threat to communities, causing loss of life and great economic losses (GINTING; MUNDANI, 2019).

The severity of dam-break disasters is associated with the release of a large mass of water instantaneously, usually in inhabited areas. It becomes relevant to study the evolution of the breach flows for the management of environmental disasters. And, the numerical simulation of a hydrodynamic model has important contributions in decision making through flooding events.

The present work deals with the numerical simulation of dam-break flow from the mathematical model based on the shallow water equations. For this, triangular finite elements with linear interpolation function are used in the spatial discretization. In time, the Characteristic-based split scheme (CBS) is applied in its explicit form, suitable for solving problems with dominant advection.

Finally, the methodology's applied to flooding situations present in the literature, making it possible to validate the adopted techniques by comparing the results obtained with publications.

## 2. THE MODEL

A two-dimensional shallow water equation system is obtained by integrating the conservation of mass and momentum equations, applying Leibniz's rule for variable boundary integrals (AWRUCH, 1983). Also, the model formulation are adopted: the specific mass is constant; the horizontal dimensions are much larger than the vertical dimensions;

the bottom topography doesn't change in time; the pressure is hydrostatically distributed; the vertical velocity is very small and its acceleration is neglected; the velocity at the bottom is null; and the horizontal components of the velocity aren't uniform, making it convenient to work with an average value that's constant with depth (ZIENKIEWICZ *et al.*, 2005). So, the shallow water equations is given by:

$$\frac{\partial h}{\partial t} + \frac{\partial U_i}{\partial x_i} = 0, \quad (1)$$

$$\frac{\partial U_i}{\partial t} + \frac{\partial F_{ij}}{\partial x_j} + \frac{g}{2} \frac{\partial \eta}{\partial x_i} \frac{\partial H}{\partial x_i} + (-1)^{i+v} U_k + \left( \frac{g}{c_m^2} \frac{|U|}{h^2} U_i \right) = \bar{c}_d |W| W_i, \quad (2)$$

in the domain  $\Omega$  with  $i, j = 1, 2$  and  $k = i + (-1)^{i+1}$ , onde  $u_i(x_1, x_2, t)$  is the component of instantaneous velocity in the  $x_i$  direction,  $U_i(x_1, x_2, t)$  is the component of flow (flow per unit width) in the direction of  $x_i$ ,  $h(x_1, x_2, t)$  is the total depth,  $H(x_1, x_2)$  is the distance from the reference plane to the bottom and  $\eta(x_1, x_2, t)$  is the elevation of the free surface relative to the reference plane. Also,  $U_i = \hat{U}_i h$ ,  $F_{ij} = \hat{U}_i U_j$ ,  $h = H + \eta$ ,  $g$  is the acceleration of gravity ( $m \cdot s^{-2}$ ),  $\hat{U}_i(x_1, x_2, t)$  is the component of velocity constant at depth in the  $x_i$  direction,  $v = 2\omega \sin \theta = 1.4 \cdot 10^{-4} \sin \theta$  is the Coriolis coefficient ( $\omega = 7 \cdot 10^{-5} s^{-1}$  is the rotational angular velocity for Earth and  $\theta$  is the latitude of the point considered),  $c_m$  is the Chezy coefficient ( $m^{1/2} s^{-1}$ ), which is linked to Manning's coefficient  $v$  by the expression  $c_m = h^{1/6} v^{-1}$  (where  $v$  is given in  $s/m^{1/3}$  and  $g/c_m^2$  is dimensionless),  $\bar{c}_d$  is a dimensionless drag coefficient,  $|W|W_1 = |W||W| \cos \vartheta$  and  $|W|W_2 = |W||W| \sin \vartheta$ , where  $|W|$  is the absolute value of the wind speed and  $\vartheta$  is the wind direction (BUKATOV; ZAV'YALOV, 2004).

In shallow water systems the wavelengths are large, due to long waves, whose celerity  $c_w$  is given by:

$$c_w \cong \sqrt{gh} \text{ or } c_w^2 = \frac{dp}{dh} = \frac{1}{c_w^2} \frac{\partial p}{\partial t},$$

where  $p$  is the pressure given by  $p = \frac{1}{2} g(h^2 - H^2)$ .

The initial and boundary conditions must be given to shallow water equations. The initial conditions consist of providing  $U$  and  $h$  values at  $t = 0 s$  and the forced boundary conditions, of Dirichlet type, are: a)  $\mathbf{Un} = U_i n_i = \mathbf{0}$  in  $\Gamma_w$  ("solid" or "closed" contour); b)  $\mathbf{Un} = U_i n_i = \bar{U}_n$  in  $\Gamma_U$  ("open" contour); c)  $h = \bar{h}$  in  $\Gamma_h$  ("open" contour).  $\bar{U}_n$  and  $\bar{h}$  are prescribed values of the unknowns in the parts  $\Gamma_U$  and  $\Gamma_h$ . And,  $n_i$  is the unit versor component. The total contour  $\Gamma$  is the union of all parts, so  $\Gamma = \Gamma_w \cup \Gamma_U \cup \Gamma_h$ .

### 3. DISCRETIZATION OF THE EQUATIONS

### 3.1 Spatial discretization

In the shallow water equations, Eq. (1) and (2), the Galerkin weighted residuals technique for the finite element method is employed, using three-node triangular elements with linear interpolation function (ZIENKIEWICZ *et al.*, 2005).

The methodology's applied to the governing equations of the flow at the level of a finite element, generic of area  $B$ . The variables are interpolated on the element with linear functions  $\underline{\phi} = [\phi_1 \ \phi_2 \ \phi_3]$  and the weighting factors are simplified. The conservation of mass and momentum equations can be compacted as:

$$\underline{M} \dot{\underline{h}} + \underline{A}_i \underline{U}_j = 0,$$

$$\underline{M} \dot{\underline{U}}_j + \underline{K}_j \underline{U}_j + \underline{K}_k \underline{U}_k + g \bar{h} \underline{A}_i \underline{h} = \underline{P}_j^U,$$

where the symbol "—" below the variable indicates a nodal quantity and above the variable

indicates the barycenter of the element,  $\dot{\underline{h}} = \frac{\partial h}{\partial t}$  and  $\dot{\underline{U}}_j = \frac{\partial U_j}{\partial t}$ ,  $\bar{h} = \underline{\phi} \underline{h} = \frac{(h_1+h_2+h_3)}{3}$

whose  $h_i (i = 1,2,3)$  are the values of  $h$  at the finite elemento nodes.

The matrices and vectors are given by:

$$\begin{aligned} \underline{M} &= \int_B (\underline{\phi}^T \underline{\phi}) dB & \underline{K}_k &= [(-1)^i v \underline{M}] \\ \underline{A}_i &= \int_B \left( \underline{\phi}^T \frac{\partial \underline{\phi}}{\partial x_i} \right) dB & \underline{K}_j &= \left[ \underline{A}_j^u + \left( \frac{g}{c_m^2} \right) \left( \frac{|\bar{U}|}{\bar{h}^2} \right) \underline{M} \right] \\ \underline{A}_j^u &= \int_B \left( \underline{\phi}^T \frac{\partial \underline{\phi}}{\partial x_j} \right) \hat{U}_j^T dB & \underline{P} &= \int_B \underline{\phi}^T dB \\ & & \underline{P}_j^U &= (\bar{c}_d |W| W_i) \underline{P} - g \bar{h} \underline{A}_i \underline{H} \end{aligned}$$

with  $i, j = 1,2$  and  $k = i + (-1)^{i+1}$ .

The finite element method (FEM) is a technique to transform a continuous problem into a discrete problem, so that the solution is obtained in a finite number of points, the element nodes. In this work, the shallow water model is applied in a two-dimensional domain, using triangular-shaped elements with nodes located at their vertices, having the coordinates and the unknowns of the problem interpolated by linear functions.

Any point located inside a triangular element with  $x$  and  $y$  coordinates is given a new dimensionless coordinate system, called triangular or natural coordinates. According to Huebner *et al.* (2001), this new coordinate system is related to the spatial coordinates by:

$$L_i = \frac{(a_i + b_i x + c_i y)}{2A}, \quad L_1 + L_2 + L_3 = 1 \quad \text{and} \quad \underline{\phi} = [L_1 \ L_2 \ L_3],$$

where  $a_i = x_j y_k - x_k y_j$ ,  $b_i = y_j - y_k$  and  $c_i = x_k - x_j$  ( $i, j, k = 1, 2, 3$  and  $i \neq j \neq k$ ).

The matrices are assembled for each element. To solve the problem, you must make the assembly for the entire system, apply the boundary and initial conditions and adopt a scheme for integration in time. After performing these steps, the unknowns,  $h$  and  $U_i$ , are calculated at each node of the mesh.

### 3.2 Time discretization

The Characteristic-based split scheme (CBS) is employed in the time integration of shallow water equations. The scheme makes a split of the problem variables, which are the components of the flow per unit width  $U_i$  (or the velocity components  $\hat{U}_i$ ) and the total depth  $h$ .

The CBS scheme is presented in detail by ZIENKIEWICZ *et al.* (2005), where the variable is obtained from the Taylor Series expansion, with time increment  $\Delta t = t^{n+1} - t^n$ . The first step of the method is to solve the momentum equation without the pressure terms by splitting it into  $\Delta U_i = \Delta U_i^* + \Delta U_i^{**}$ , whose pressure is considered as a source term in  $\Delta U_i^{**}$ . After calculating  $\Delta U_i^*$ , the pressure is calculated. In the last step,  $\Delta U_i$  is determined, in order to obtain the average flow  $U_i^{n+1}$  evaluated at time  $n + 1$  by means of  $U_i^{n+1} = U_i^n + \Delta U_i$ .

The three-step procedure can be solved explicitly or implicitly, in this paper a fully explicit scheme is employed. Therefore, the stability condition is that the time step adopted is less than or equal to the critical time interval. That is,  $\Delta t \leq \Delta t_{crit}$ , where  $\Delta t_{crit} = \frac{l}{c_w + |U_i|}$ , whose  $l$  is a characteristic size of the element (GRAVE, 2016).

In this way the time discretization of the equations obtained with the application of finite elements is done. So:

Step 1:

$$\left( \underline{M}_D \underline{\Delta U}_i^* \right)^{m+1} = -\Delta t \left\{ \left[ \left( \underline{A}_j^u + \underline{M}^\beta \right) \underline{U}_i + \underline{M}^v \underline{U}_k + \underline{A}_i^H \underline{H} - \underline{P}_i^w \right] - \frac{\Delta t}{2} \left[ \left( -\underline{D}_{kj}^u + \underline{A}_k^{u,\beta} \right) \underline{U}_i + \underline{A}_k^{u,v} \underline{U}_s - \underline{D}_{ki}^{u,w} \underline{H} - \underline{P}_{k,i}^w + \underline{f}_{kj}^u \right] \right\}^n + \left( \underline{M}_D - \underline{M} \right) \left( \underline{\Delta U}_i^* \right)^m.$$

Step 2:

$$\left( \frac{\bar{h}}{c_w^2} \underline{M}_D \underline{\Delta p} \right)^{m+1} = -\Delta t \left\{ \underline{A}_j \left( \underline{U}_j + \frac{1}{2} \underline{\Delta U}_j^* \right) - \frac{\Delta t}{2} \bar{h} \left( -\underline{D}_{kj}' \underline{p} + \underline{f}_p \right) \right\}^n + \frac{1}{c_w^2} \left( \underline{M}_D - \underline{M} \right) \underline{\Delta p}^m$$

Step 3:

$$(\underline{M}_D \underline{\Delta U}_j)^{m+1} = -\underline{M} \underline{\Delta U}_j - \Delta t \bar{h} \left[ \underline{A}_i \underline{p} - \frac{\Delta t}{2} \left( -\underline{D}_{ki}^u \underline{p} + \underline{f}_p^u \right) \right]^n + (\underline{M}_D - \underline{M}) (\underline{\Delta U}_j)^m.$$

Final variable calculations:

$$\begin{aligned} \underline{U}_j^{n+1} &= \underline{U}_j^n + \underline{\Delta U}_j & \underline{p}^{n+1} &= \underline{p}^n + \underline{\Delta p} \\ \underline{h}^{n+1} &= \left[ \underline{H}^2 + \frac{2p}{g} \right]^{\frac{1}{2}} & \underline{\hat{U}}_i^{n+1} &= \frac{\underline{U}_i^{n+1}}{\underline{h}^{n+1}}, \end{aligned}$$

with  $i, j, k = 1, 2$  and  $s = i + (-1)^{i+1}$ ,  $m$  is the iterations number and  $n$  is the time instant.

The matrices and vectors are:

$$\begin{aligned} \underline{M} &= \int_{\Omega} \underline{\phi}^T \underline{\phi} d\Omega & \underline{M}^v &= v' \underline{M} & \underline{M}^\beta &= \beta \underline{M} \\ \underline{M}_D &= \frac{\Omega}{3} \underline{I} & \underline{A}_j &= \int_{\Omega} \left( \underline{\phi}^T \frac{\partial \underline{\phi}}{\partial x_j} \right) d\Omega & \underline{A}_j^u &= \int_{\Omega} \underline{\phi}^T \left( \frac{\partial \underline{\phi}}{\partial x_j} \underline{\hat{U}}_j \right) d\Omega \\ \underline{A}_k^{u,\beta} &= \int_{\Omega} \underline{\phi}^T \left( \underline{\hat{U}}_k \frac{\partial \underline{\phi}}{\partial x_k} \right) d\Omega & \underline{A}_k^{u,v} &= v' \int_{\Omega} \underline{\phi}^T \left( \underline{\hat{U}}_k \frac{\partial \underline{\phi}}{\partial x_k} \right) d\Omega & \underline{A}_i^H &= g \eta \int_{\Omega} \left( \underline{\phi}^T \frac{\partial \underline{\phi}}{\partial x_i} \right) d\Omega \\ \underline{P}_i^w &= \gamma_i \int_{\Omega} \underline{\phi}^T d\Omega & \underline{P}_k' &= \int_{\Omega} \frac{\partial \underline{\phi}^T}{\partial x_k} d\Omega & \underline{P}_{k,i}^{u,w} &= \gamma_i \int_{\Omega} \frac{\partial (\underline{\hat{U}}_k \underline{\phi}^T)}{\partial x_k} d\Omega \\ \underline{D}_{kj}' &= \int_{\Omega} \frac{\partial \underline{\phi}^T}{\partial x_k} \frac{\partial \underline{\phi}}{\partial x_j} d\Omega & \underline{D}_{kj}^u &= \int_{\Omega} \frac{\partial (\underline{\hat{U}}_k \underline{\phi}^T)}{\partial x_k} \frac{\partial (\underline{\hat{U}}_j \underline{\phi})}{\partial x_j} d\Omega & \underline{D}_{ki}^{u,H} &= g \eta \int_{\Omega} \frac{\partial (\underline{\hat{U}}_k \underline{\phi}^T)}{\partial x_k} \frac{\partial \underline{\phi}}{\partial x_i} d\Omega \\ \underline{f} &= \int_{\Gamma} \underline{\phi}^T q_n^p d\Gamma & \beta &= \frac{g |\underline{U}|}{c_m^2 \bar{h}^2} \\ \gamma_i &= \bar{c}_d |W| W_i \end{aligned}$$

$$\underline{f}_{kj}^u = \int_{\Gamma} \left( \underline{\hat{U}}_k \underline{\phi}^T \right) \frac{\partial (\underline{\hat{U}}_j \underline{\phi})}{\partial x_j} n_j d\Gamma = \int_{\Gamma} \left( \underline{\hat{U}}_k \underline{\phi}^T \right) q_n^u d\Gamma \quad \underline{f}_{-p}^u = \int_{\Gamma} \left( \underline{\hat{U}}_k \underline{\phi}^T \right) \frac{\partial (\underline{\phi} p)}{\partial x_j} n_j d\Gamma = \int_{\Gamma} \left( \underline{\hat{U}}_k \underline{\phi}^T \right) q_n^p d\Gamma$$

$$q_n^u = \frac{\partial (\underline{\hat{U}}_j)}{\partial x_n} = \left[ \frac{\partial (\underline{\phi} \underline{\hat{U}}_j)}{\partial x_j} \right] n_j \quad q_n^p = \frac{\partial p}{\partial x_n} = \left[ \frac{\partial (\underline{\phi} p)}{\partial x_j} \right] n_j$$

$$\underline{D}_{kj}^u(m, n) = \underline{D}_{kj}'[(m), (n)] \underline{\hat{U}}_k[(m)] \underline{\hat{U}}_j[(n)] \quad \underline{P}_{k,i}^{u,w}(n) = \underline{P}_k'[(n)] \underline{U}_k[(n)]$$

$$\underline{A}_k^{u,\beta}(m, n) = \beta \underline{\hat{U}}_k[(n)] \underline{A}_k[m, (n)] \quad \underline{A}_k^{u,v}(m, n) = \bar{v} \underline{\hat{U}}_k[(n)] \underline{A}_k[m, (n)]$$

where  $\underline{I}$  is the identity matrix,  $v' = (-1)^i v$ ,  $\bar{\eta} = \bar{h} - \bar{H}$  and  $ij, k = 1, 2$ .

## 4. RESULTS AND DISCUSSION

A computational code was developed by GRAVE (2016) in FORTRAN language, solving the shallow water equations by FEM and the CBS scheme. To numerically simulate a real situation a tool is needed to modify the domain as the water resource level varies causing floods and droughts, introducing or extracting elements in the domain, working with the idea of "dry" and "wet" elements, varying with time.

Therefore, it's relevant to know which mesh elements belong to the boundary between a dry ( $h = 0$ ) and a wet ( $h > 0$ ) region. The equations can't be solved directly if  $h = 0$ . For this reason, two types of nodes and elements can be distinguished: "dry" nodes ( $h = h_{min}$ ) and "wet" nodes ( $h > h_{min}$ ), where  $h_{min}$  is the minimum water level adopted as reference. The "dry" elements are those that have one or two "dry" nodes, while the "wet" elements have all their nodes "wet". And, in the numerical algorithm only the "wet" nodes and elements are considered (GRAVE, 2016).

The methodology presented is applied to solve dam-break cases from the literature, with results available for comparison. The simulations of the examples demanded the replication of the computational meshes, with the number of triangular finite elements, the boundary conditions and the parameters used from the literature.

### 4.1 Partial break on wet bed

The partial dam-break over the wet bed is an example used to examine the shock capturing capability in shallow water models, as simulated by PARSA (2018).

The study domain is represented is a  $200 \times 200 \text{ m}^2$  mesh, this geometry is illustrated in Figure 1. The computational mesh consists of 4,892 nodes and 9,424 triangular elements and the wall boundary condition. To limit the dry or wet areas the value of  $h_{min} = 0.01 \text{ m}$  and the acceleration of gravity of  $9.8 \text{ m/s}^2$  was assigned. The initial condition ( $t = 0 \text{ s}$ ), the water height inside the reservoir is 10 and 5 m in the outer region. Coriolis effects, wind action and bottom friction are neglected in this test case.

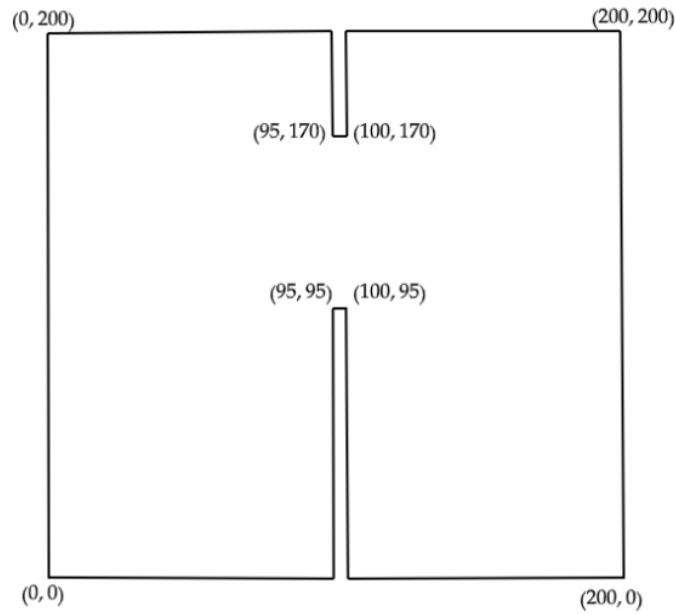


**Figure 1.** Partial break on wet bed: Geometry

**Source.** Authors' elaboration

Figures 2 and 3 show the results in three-dimensional and two-dimensional form, respectively, at 7.2 s. With the dam-break the water flow moves towards the outer region, producing waves downstream where the water level rises. While, there is progressive emptying upstream due to negative waves. It's observed that the results generated in comparison with PARSA (2018) are satisfactory.

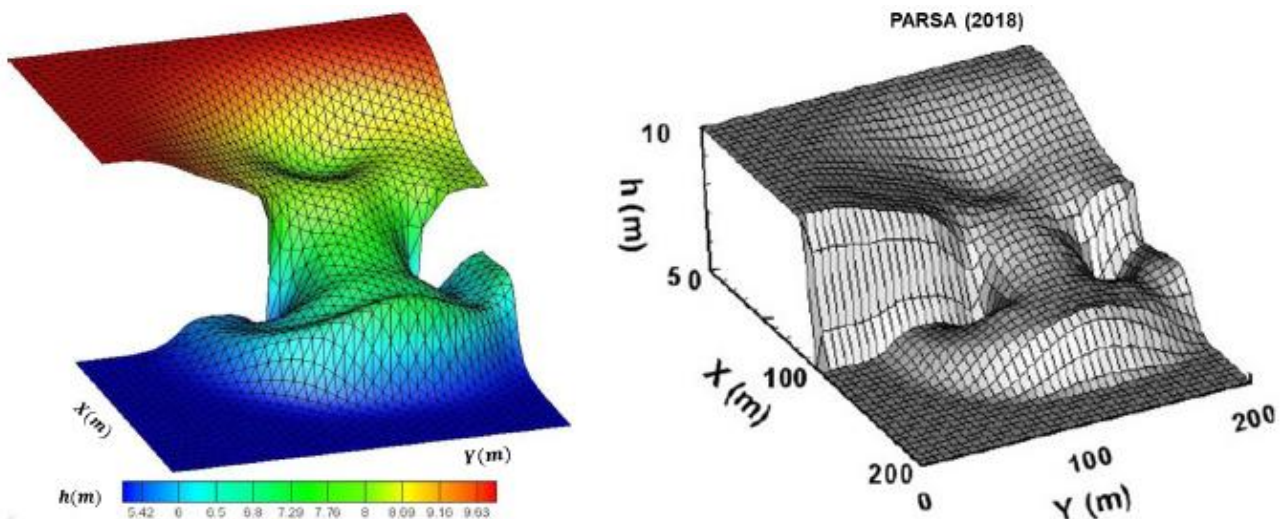


**Figure 2.** Partial break on wet bed: Surface profile at 7.2 s



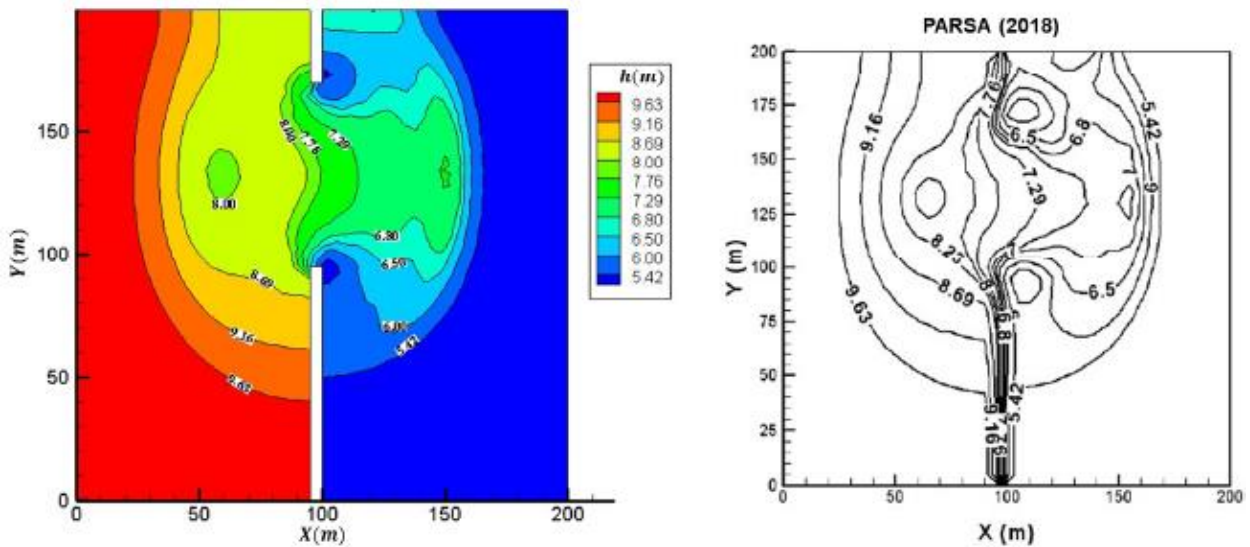


Figure 3. Partial break on wet bed: Contour lines at 7.2 s

#### 4.2 Flow against two solid obstacles

Flooding in urban areas occurs with the flow of water between buildings. It's necessary to consider the presence of solid obstacles to simulate events of this type, analyzing their influence on runoff. The example approached by PENG (2012) is reproduced in comparison with experimental results.

The study region is a  $1.6 \times 0.6 \text{ m}$  rectangular flume, characterizing a closed reservoir with two square columns, with dimension  $0.1 \text{ m}$  and height  $0.3 \text{ m}$ , at  $x = 1.2 \text{ m}$ . Because the natural channel isn't as flat as the artificial construction, six small square obstacles are added to the side walls, at  $x = 0.4, 0.8 \text{ and } 1.2 \text{ m}$  to simulate the irregular banks. More details of the geometry can be observed in Figure 4.

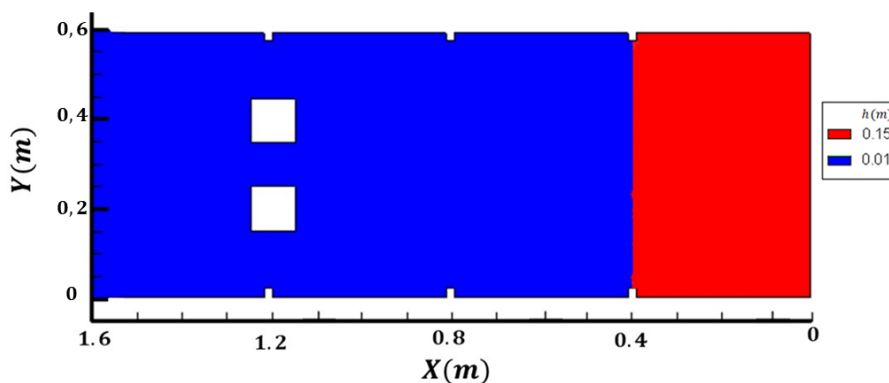


Figure 4. Flow against two solid obstacles: geometry

Source: Authors' elaboration

The present test case adopts the hypothesis of the existence of a gate, holding back the fluid at  $x = 0.4 \text{ m}$ , which when removed quickly causes the dam-break flow. The initial condition of the problem is also shown in Figure 4, where the water level prior to the gate is  $x = 0.15 \text{ m}$  and from it's  $x = 0.01 \text{ m}$ .

The solid obstacles representation is done by the vertical walls technique, described by GRAVE (2016). The methodology consists in making "holes" in the mesh where the objects are located, being applied the wall boundary condition to close the boundaries and characterize the buildings, preventing the flow from advancing over the obstacle. The technique is adopted since in the urban area the runoff occurs between buildings, except in the case of large tsunamis.

The computational mesh has 4,892 nodes and 9,424 triangular elements, with the closed boundary condition. The Manning coefficient is  $x = 0.01 \text{ s/m}^{\frac{1}{3}}$ , the acceleration of gravity is  $9.806 \text{ m/s}^2$  and  $h_{min}$  is  $0.01 \text{ m}$  to limit the dry or wet areas. Wind action and Coriolis effect are neglected.

The results obtained from the model are compared with the solutions presented by PENG (2012). The total simulation time of the flow is  $2 \text{ s}$ , from opening to the return of the wave to the gate. In Figure 5 it's observed that it takes approximately  $0.56 \text{ s}$  for the wave to reach the square columns, traveling about  $0.8 \text{ m}$ , in addition to the influence of the side objects.

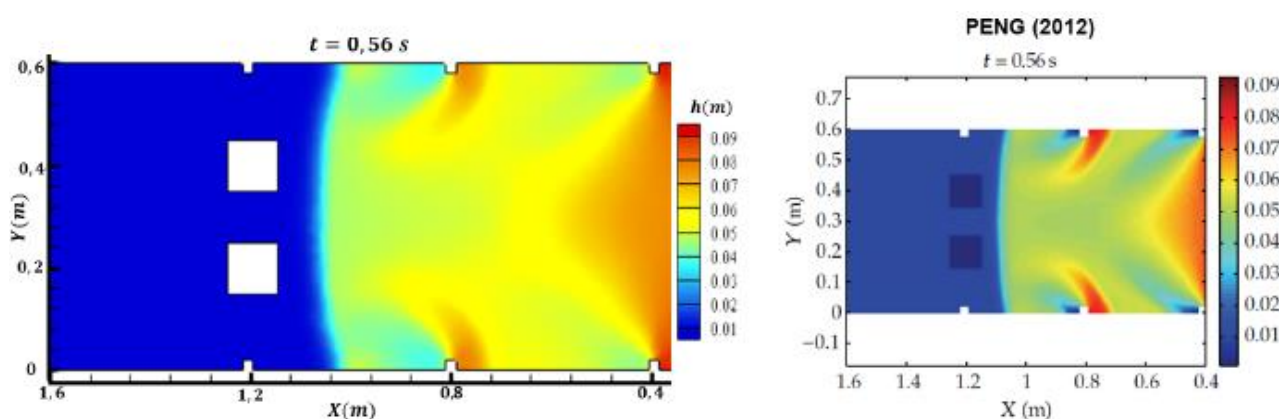


**Figure 5.** Flow against two solid obstacles: comparison of solutions at  $t = 0.56 \text{ s}$

The flow from the dam-break is directed into the space between the solid obstacles in Figure 6, and the water level rises by reflection with the face of the columns. Next, in Figure 7, at  $0.725 \text{ s}$  the wave envelops the columns and forms vortices.

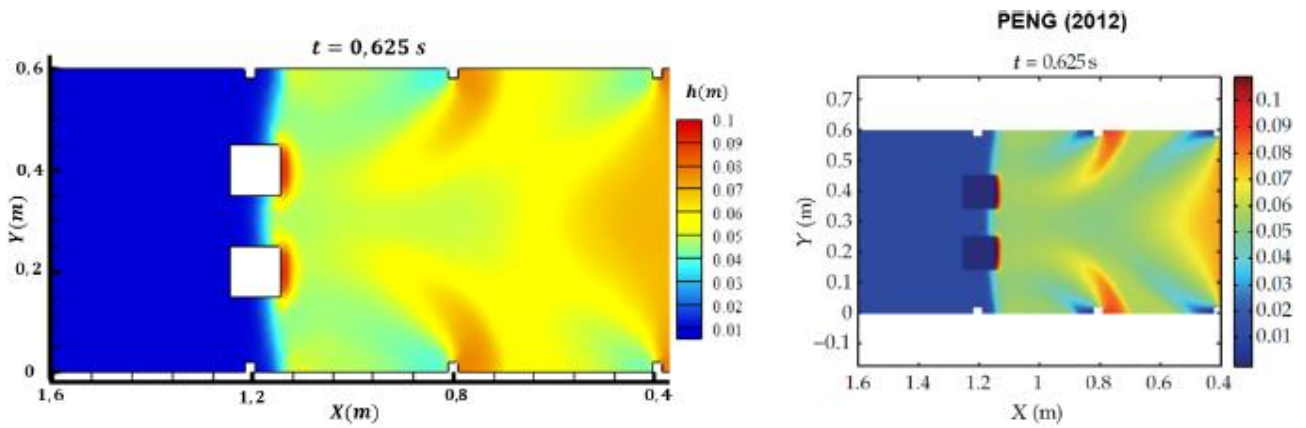


Figure 6. Flow against two solid obstacles: comparison of solutions at  $t = 0.625$  s

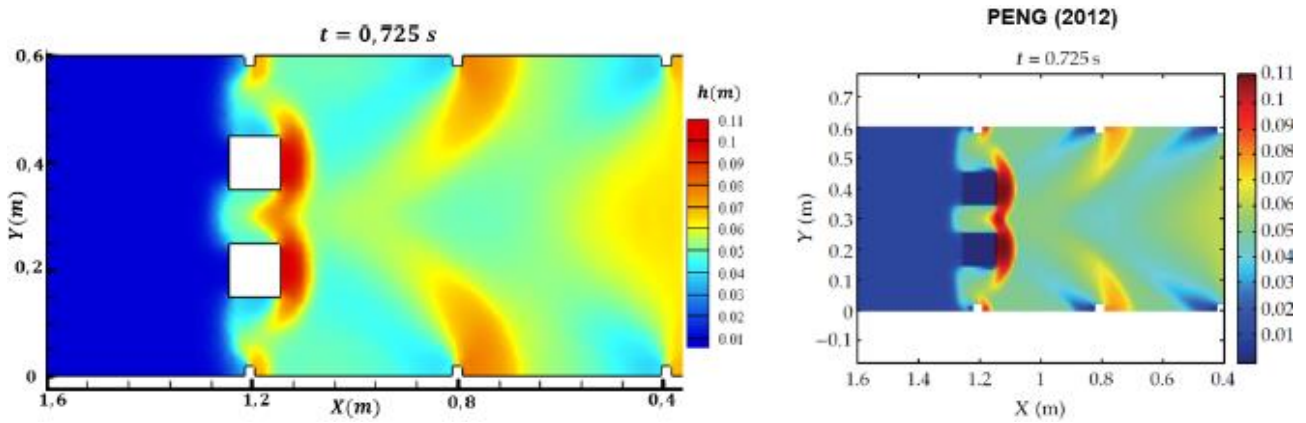


Figure 7. Flow against two solid obstacles: comparison of solutions at  $t = 0.725$  s

Finally, in Figure 8 the flow approaches the domain boundary at 0.925 s, with the waves returning toward the gate at 1.75 s, in Figure 9, there being a change in the direction of the flow.

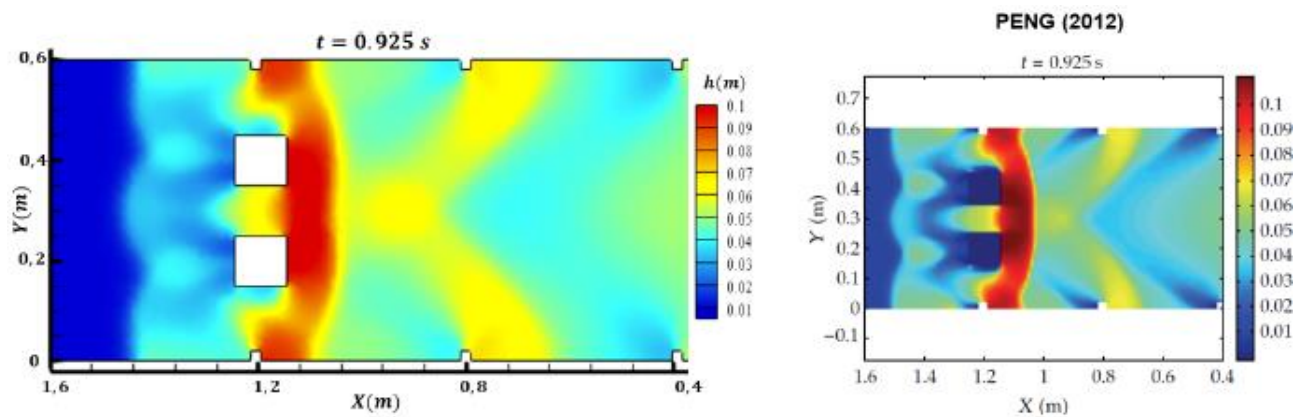
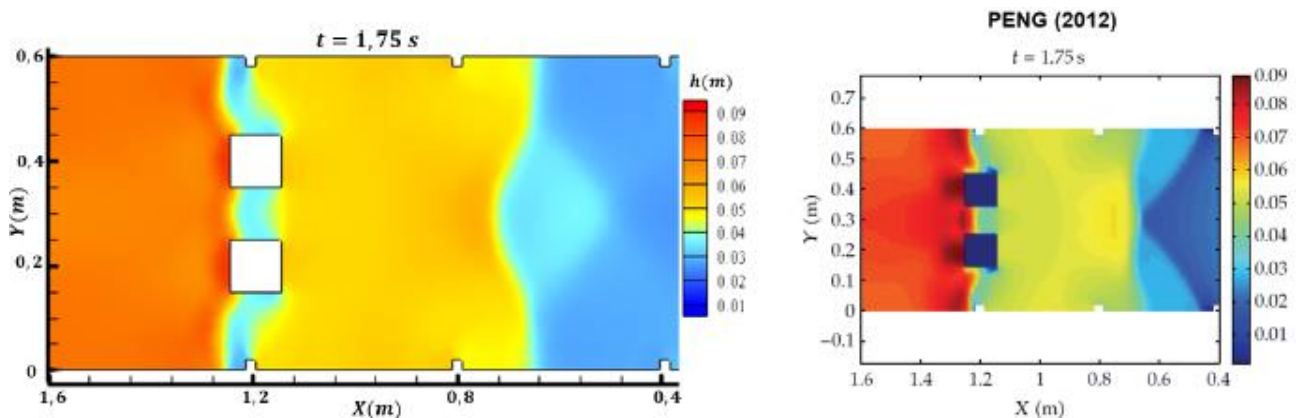


Figure 8. Flow against two solid obstacles: comparison of solutions at  $t = 0.925$  s



**Figure 9.** Flow against two solid obstacles: comparison of solutions at  $t = 1.75$  s

The model captured the wave formation due to the gate opening and the contact with the solid walls, of both columns and the side obstacles. The results make it known that flow occurs with the presence of obstacles, as in the urban area. The results compared to PENG (2012) were satisfactory.

## 5. CONCLUSIONS

This paper proposes the numerical solution of the two-dimensional shallow water mathematical model with the finite element method and the CBS scheme. The methodology showed satisfactory performance in simulating different examples of dam-break, capturing the oscillations from the sudden flow and the change of motion.

In the example of partial dam-break on wet bed, the contour lines are similar to the results presented in the literature, identifying the significant difference between the height ( $h$ ) inside and outside the reservoir. In the second example, flow against two solid obstacles, the results highlighted the influence through the flow as it occurs in flooding events in the urban area.

Finally, the numerical simulation with the shallow water model provides an opportunity for contributions in the representation of dam-break flows, providing perspectives on the occurrence of this type of disaster and projections of its scope.

In future work it will be possible to associate the hydrodynamic model with real flooding and pollutant dispersion events. The mathematical modeling provides several future perspectives for studies in the area of environmental disasters.

## REFERENCES

- Awruch, A. M. **Modelos numéricos em hidrodinâmica e fenômenos de transporte usando o método dos elementos finitos**. Thesis (Doctoral Course) - Federal University of Rio de Janeiro, 1983. Available at: <<https://buscaintegrada.ufrj.br/Record/aleph-UFR01-000159281>>. Accessed on: 15 feb. 2022.
- Bukatov, A. E.; Zav'yalov, D. D. Wind-induced motion of water in shallow-water closed basins. **Physical Oceanography**. Berlin, v. 14, n. 5, p. 284-294, 2004.
- Cardoso, F. C. O. **Um modelo matemático para o controle de poluição das águas**. Dissertation (Master's Course) – Federal University of Rio Grande do Sul, 1980. Available at: <<https://lume.ufrgs.br/handle/10183/132684>>. Accessed on: 15 feb. 2022.
- Ginting, B. M.; Mundani, R. P. Comparison of shallow water solvers: Applications for dam-break and tsunami cases with reordering strategy for efficient vectorization on modern hardware. **Water**. Basel, v. 11, n. 639, p.1-31, 2019.
- Grave, M. **Simulação e Controle de Enchentes Usando as Equações de Águas Rasas e a Teoria do Controle Ótimo**. Dissertation (Master's Course) – Federal University of Rio Grande do Sul, 2016. Available at: <<https://www.lume.ufrgs.br/handle/10183/134560>>. Accessed on: 15 feb. 2022.
- Parsa, J. Characteristic Based Split Finite Element for Unsteady Dam-Break Problem. **Journal of Hydraulic Structures**. Khuzestan: v. 4, n. 2, p. 27-41, 2018.
- Peng, S. H. 1D and 2D numerical modeling for solving dam-break flow problems using finite volume method. **Journal of Applied Mathematics**. London, v. 2012, p. 1-14, 2012.
- Zienkiewicz, O. C.; Taylor, R. L. and Nithiarasu, P. **Finite Element Method for Fluid Dynamics**. v.2. 6. ed.Oxford: Butterworth-Heinemann, 2005.